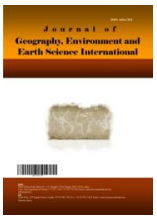

Journal of Geography, Environment and Earth Science International

24(8): 11-25, 2020; Article no.JGEESI.63120
ISSN: 2454-7352

Contribution of Sentinel Radar Images 1Ato the Extraction of Lineaments from the Lobo Watershed (Center-West of the Ivory Coast)

J. O. K. Kouadio[1*], B. Dibi[1], M. J. Mangoua[1], A. B. Konan-Waidhet[1] and B. Kamagaté[2]

[1]UFR Environment, Laboratory of Environmental Sciences and Technologies, Jean Lorougnon Guedé Daloa University, BP 150 Daloa, Côte d'Ivoire.
[2]UFR Sciences and Environmental Management (SGE), Geosciences and Environment Laboratory, Nangui Abrogoua University, 02 BP 801 Abidjan 02, Côte d'Ivoire.

Authors' contributions

This work was carried out in collaboration among all authors. Author JOKK designed the study, performed the statistical analysis, wrote the protocol and wrote the first draft of the manuscript. Authors BD and MJM managed the analyses of the study. Authors ABKW and BK managed the literature searches. All authors read and approved the final manuscript.

Article Information

DOI: 10.9734/JGEESI/2020/v24i830245
Editor(s):
(1) Prof. Anthony R. Lupo, University of Missouri, USA.
Reviewers:
(1) Amardeep Singh, CSMRS, India.
(2) Mahmoud Ali Refaey Eltoukhy, Benha University, Egypt.
(3) Muzher Mahdi Ibrahem Aldoury, Tikrit University, Iraq.
Complete Peer review History: http://www.sdiarticle4.com/review-history/63120

Original Research Article

Received 20 September 2020
Accepted 24 November 2020
Published 03 December 2020

ABSTRACT

The improvement of the conditions of access to drinking water for the populations of the Lobo watershed requires the exploitation of groundwater because of the surface water which remains exposed to climatic hazards and the impacts of anthropic activities. And yet, these underground waters finds himself bedrock aquifer which are complex aquifers. Thus, the objective of this study is to characterize those fissure aquifers that who govern underground run-off in the aquifer system of the Lobo catchment area. The methodology adopted consisted in using 1A sentinel radar images to map fractures and their spatial distribution. The validation of the lineaments first consisted in comparing and highlighting the lineaments from the radar images and the fractures revealed from photo-geological images. Next, we superimposed the map of lineaments on the map of boreholes

**Corresponding author: E-mail: olivierkouame05@gmail.com;*

with a flow rate greater than or equal to 5 m^3/h, which were considered as productive boreholes. To determine the traffic corridors, this fracturing map was superimposed on the piezometric map. This work made it possible to extract 9,753 lineaments over a surface area of 7,000 km². The various validation techniques enabled us to confirm 121 major fractures with an average length of 9 km. In addition, the most productive boreholes are located on average less than 300 m from the fractures. The analysis of the distribution of the orientations of these fractures revealed a heterogeneity of direction and a predominance of the N-S; NW-SE and NE-SW families. The Fracturing density maps and density of the number of fracture crossing points highlight the spatial heterogeneity of the fracture network which is controlled by geomorphology, geological formations and lithological contacts. The river Lobo and its main tributary the Dé, flow preferentially in fractures. This river and its tributary drains the aquifer system. The results obtained from different thematic maps are useful for the realisation of future high-yield hydraulic wells ($Q \geq 5$ m^3/h).

Keywords: Aquifer; fracture network; lineaments.

1. INTRODUCTION

Groundwater resources in rock aquifers represent a major resource for rural populations south of the Sahara because surface water is not perennial due to the high value of evapotranspiration or their poor quality. As the only source of quality drinking water, this groundwater conditions the food security of these populations. They are perceived as an alternative source of water due to the scarcity of surface water [1]. The response of aquifers to these different withdrawals is still poorly perceived, mainly because of their complexity. Among theses reservoirs that contain these groundwater bedrock aquifers have been constitute a problematic of growing interest since the 1960s.

In addition to the low productivity of this type of aquifer, their heterogeneous character has long been considered to be an obstacle to the prediction of their hydrodynamic properties on a local and catchment scale [2]. Fractures that affect the healthy rock play an important role in the hydrogeological characterization of groundwater [3,4,5,6] in Côte d'Ivoire, the design of the GIS in the field of groundwater research using aerial photography was initiated by [7] and made it possible to map many regional accidents. This map served as a support for various hydrogeological prospecting. Nevertheless, these aerial photographs, which were used as a support for the fracture survey, are not easy to interpret because of the vegetation and the thick layer of alteration that masks the healthy rock.

To remedy these problems, several authors [8,9,10,11,12,13,14,15,16,17] have used passive remote sensing (use of Landsat and SPOT images) to survey lineaments in different regions of Côte d'Ivoire. One of the major drawbacks of passive remote sensing is linked to the very quality of images in humid tropical zones, due to frequent cloudy atmospheric conditions that make it difficult to detect lineaments [18]. Consequently, radar images that have shown their ability to extract on a large scale and map lineaments appear to be the most suitable [19]. In addition, they use radar waves, which are more suitable for humid tropical areas since they are not affected by atmospheric scattering.

Due to their high sensitivity to surface characteristics such as roughness and moisture, radar data are particularly effective for mapping linear structures corresponding to faults, fractures and lithological contacts [20]. The objective of this study is to characterize those fissure aquifers that who govern underground run-off in the aquifer system of the Lobo watershed.

Thus, the information obtained from the 1A sentinel radar images can be used to guide future hydrogeological studies and contribute to the implementation of water resource management tools.

2. MATERIALS AND METHODS

2.1 Study Area

Located in the Centre-West of Côte d'Ivoire, the Lobo watershed lies between 6°05' and 6°55' West longitude and between 6°02' and 7°55' North latitude (Fig. 1). This zone is circumscribed in the regions of upper Sassandra whose chief town is Daloa and part of that of the Worodougou (Seguela). This basin is home to the third largest city in the Ivory Coast (Daloa), which is its economic hub. In Nibéhibé, this watershed has a

surface area of 7,000 Km². This basin is drained by the Lobo River and its main tributary the Dé. The average rainfall over the period 1971-2017 is about 1,200 mm and the average temperature is 25°C (Fig. 2).

2.2 Geographical Context

The geological formations of the Lobo watershed are dominated by two geological entities. These are the magmatic rocks which consist mainly of granit of granodiorite, diorite and tonalite. They occupy almost the entire surface of the basin. The second entity corresponds to metamorphic rocks consisting mainly of schists and migmatites (Fig. 3) [21]. These geological formations are covered by mainly ferralitic, moderately desaturated soils, made up of sands and clays.

2.3 Data

2.3.1 Wells data

A total of 133 boreholes were used for the analysis of the productivity of the cracked aquifer. These drilling data come from the Territorial Directorate of Human Hydraulics of Daloa.

2.3.2 Map data

Map data is essentially composed of:

- Geological maps of the square degrees of Daloa and Séguéla [21], from the Ivory Coast mining company (SODEMI);
- Map of major lineaments at the scale of Côte d'Ivoire, extracted by [7], from photogeological images.
- Map of the major lineaments of the Lobo watershed, extracted by [14], based on Landsat 7 images.

2.3.3 Satellite images data

The satellite images used in this study consist mainly of SAR / Sentinel 1A radar images. These images were uploaded in February 2018 on the following site:https://vertex.daac.asf.alaska.edu. The characteristics of the satellite images are summarized in Table 1. These images were previously processed (radiometric calibration, restoration of orientation).

2.4 Material

The processing of satellite images for mapping the lineaments of the Lobo watershed was carried out using SNAP software.

The ArcGis software was used to produce the various thematic maps.

Linwin software was used for the statistical analysis of the fractures.

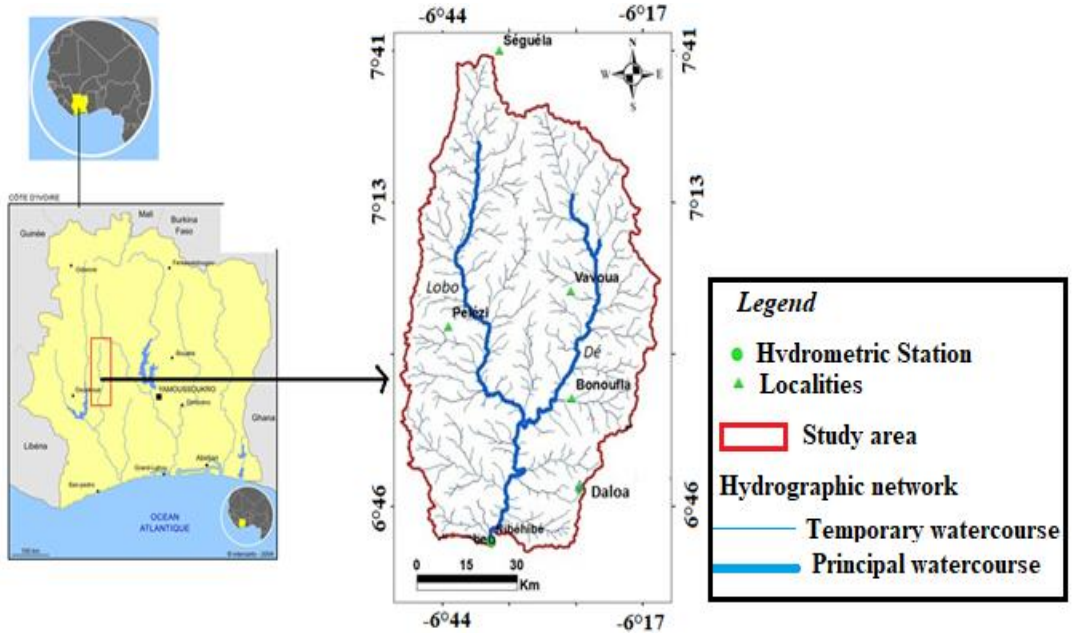

Fig. 1. Location of the Lobo catchment area (Nibéhibé)

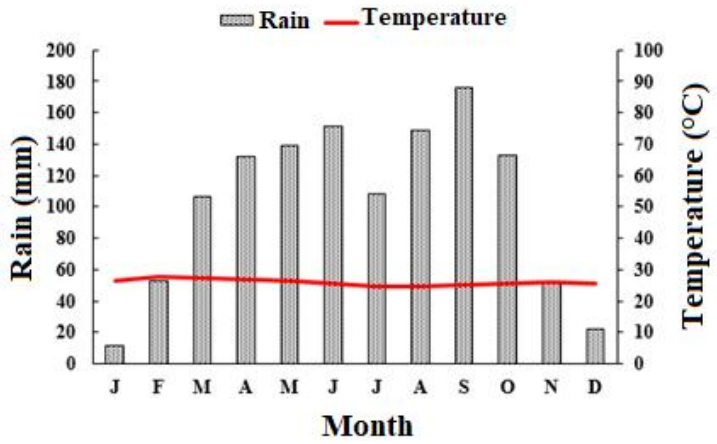

Fig. 2. Monthly evolution of rain and temperature at Daloa station (1971-2016)

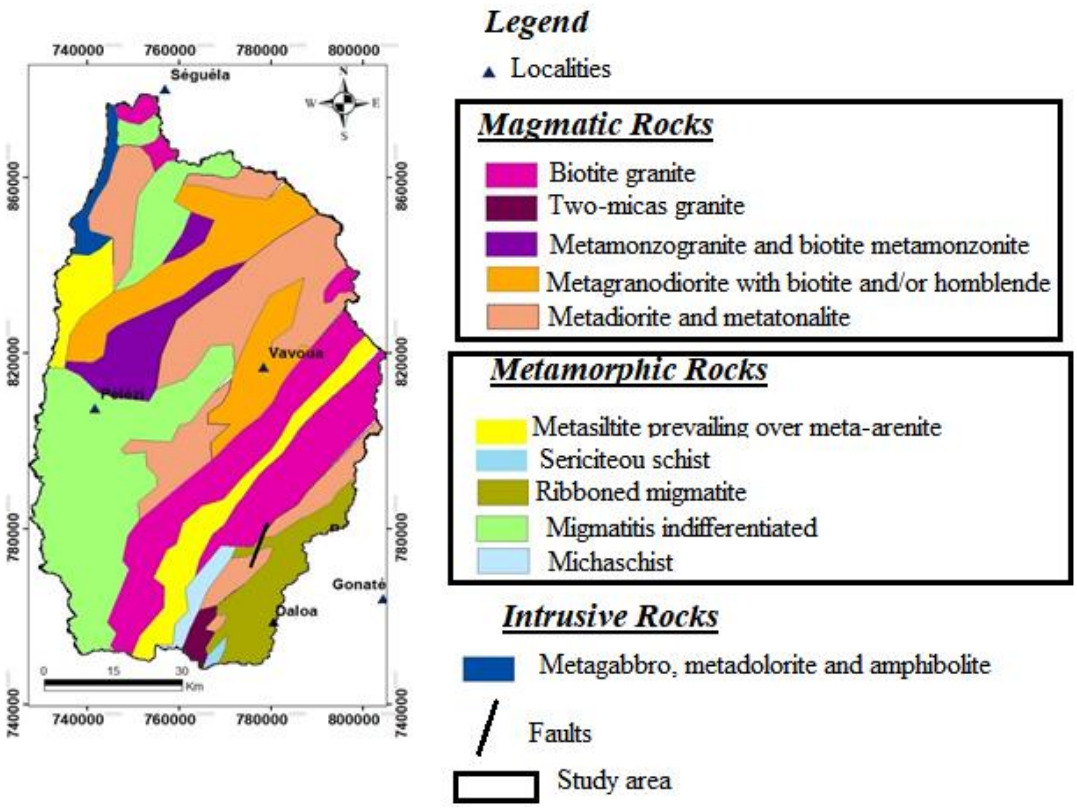

Fig. 3. Simplified geological map Lobo watershed (modified from [21]

Table 1. Characteristics of sentinel radar images 1A

Sensors	Date	Mode	Bande	Format	Broke	Spatial resolution
SAR (Polarisation VV-VH)	01/02/2018	IW1 (Interferometric Wide swath).	C (λ = 5,6 cm)	GRD (Ground Range Detected).	250 Km	10 m

2.5 Methodology

2.5.1 Mapping of geological structures

- ✓ **Radar image processing**

Sentinel 1A radar images from the SAR system were used for mapping the lineaments of the Lobo watershed.

2.5.1.1 Speckle reduction and visual images' improvement

The objective of this step is to improve the quality of these images which are affected by a lot of noise (Fig. 4). Raw radar images are affected by noises which degrade the radiometric resolution of the image. This reduces the possibility of discriminating structures, the finest mainly. Adaptive filters of Lee [22,23] and median [24] were used for noises processing. These filters maintain the sharpness and detail of the image while making noises stop (Fig. 5). The extraction of lineament was made after application of adaptive filters.

2.5.1.2 Lineaments extraction

Lineaments was derived from filtered images manually, following a visual analysis on screen. The extraction technique applied on sentinel 1A images is illustrated by Fig. 6. We digitized linear anthropogenic discontinuities such as roads, paths. These elements related to human activities are quite dynamic. It is judicious to derive them from images whose acquisition dates are recent, compare to images used for structural mapping. The anthropogenic features are not taken into account when mapping structural lineaments. To do this, the vector file of anthropogenic lineaments is alternately superimposed and then removed from the radar image, during the extraction of structural lineaments.The lineaments were extracted manually after a visual analysis of the image. In this study, lineaments longer than 9 km are referred to as major lineaments, according to work by [25] and [26].

2.5.1.3 Lineaments validation

Lineaments validation consisted in comparing and emphasizing possible matches between directions of lineaments mapped from radar images and those from previous works [7,14]. Next, we superimposed the lineament map on the map of boreholes with a flow rate greater than or equal to 5 m^3/h, which were considered as productive boreholes because they are supposed to have encountered or are closer to a fracture [27,28,19].

2.5.1.4 Relationship between fracturing and wells

Scripts designed by [29], were used to calculate the well-lineament distances. The analysis of the distance separating a well from the nearest lineament was also undertaken for validation approach issue. The distance between a wells and the nearest lineament is an important factor for plausible lineament and fracture compliance. Depending on the distance from well to the nearest lineament, the frequency of implanted well is evaluated. The wells were classified according to their yield and from the classification of 'Comité Inter-africain d'étude Hydraulique (C.I.E.H) [30], was used:

- Low yield (Q < 2,5 m^3/h);
- Medium yield (2,5 m^3/h Q < 5 m^3/h);
- High yield (Q ≥ 5 m^3/h).

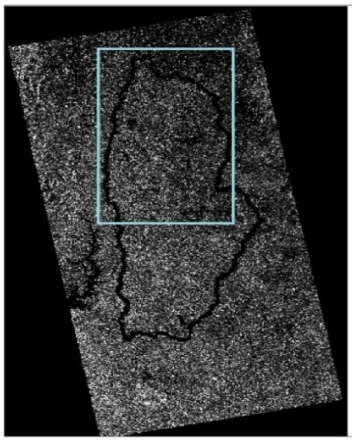

Fig. 4. Corrected raw image

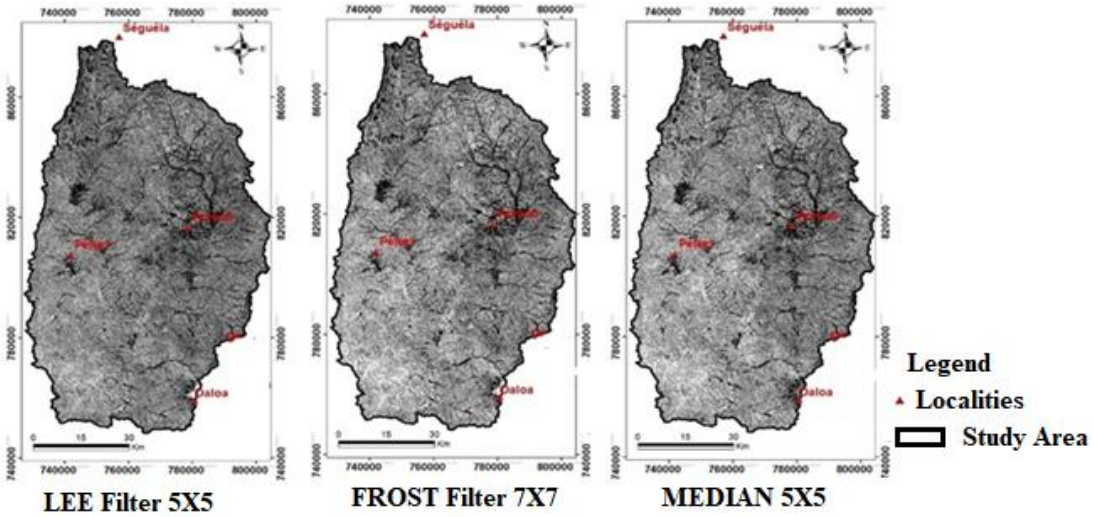

Fig. 5. Filtered radar images

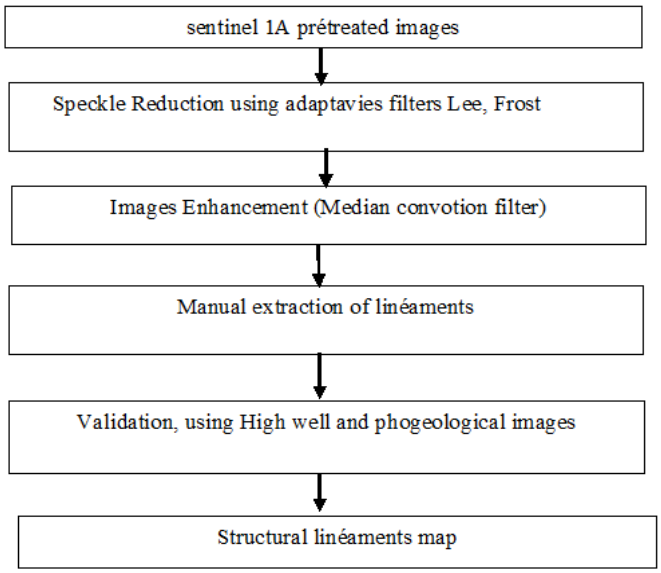

Fig. 6. Process of geological structures mapping, from radar images (radar/ Sentinel 1A)

2.5.1.5 Lineaments orientationand density studies

Lineaments'orientations are divided into class of 10 degrees and represented by circular histograms. Scripts designed by [29], were used to calculate the densities within circular mesh. The method for evaluating lineaments density is developed by [29]. For mesh construction, the lineaments map is inscribed into a rectangle and a grid of equidistant points is drawnwithin the rectangle (Fig. 7). The mesh can be circular or quadrangular. For circular mesh adopted in this current study, every point is the center for a circle of radius r corresponding to equidistance between points. According to [29], the quadrangular mesh introduces bias into the lineament density map while the circular mesh reduces bias, especially those related to orientations of lineaments. A radius r of 2 km was used to conduct the study because that value provides good mesh refinement on the rectangular area delimiting the lineament map (Fig. 7a).

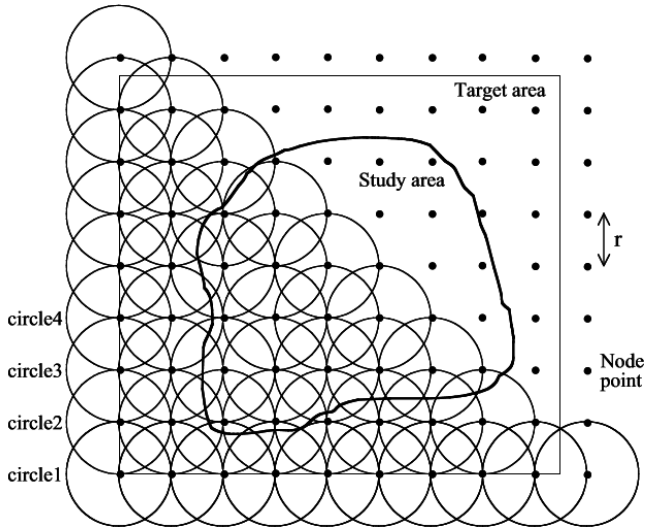

Fig. 7a. Arrangement of squared nodes and related circles with radius r and intervalr [29]

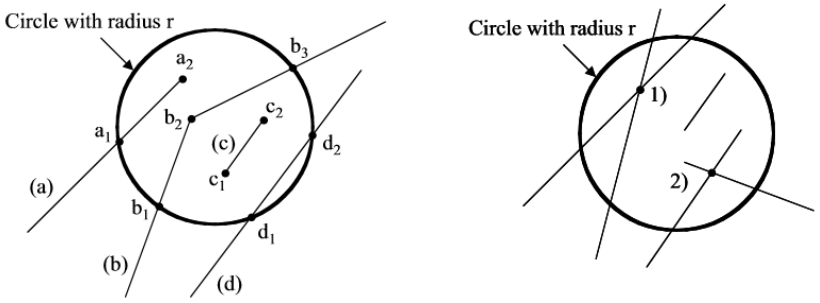

Fig. 7b. Calculation method of total length and cross-points of lineaments in a circle [29]

The assessment procedure of lineaments cumulative length and number of lineaments cross-points within each circle is highlighted in Fig. 7b. If the lineament meets the circle at two points, the distance (d1d2) is considered as the length of the lineament. In the case the lineament intercepts only one point of the circle, the lineament length is given by the distance (b2b3). Interpolations using the kriging method have been made to produce iso-value maps of cumulative length and cross-points densities.

2.5.1.6 Determination of piezometric levels

In order to assess the impact of fracturing on the circulation of groundwater, a piezometric map has been carried out. Indeed, this map schematises the reservoir's driving function and the hydrodynamic behaviour of the aquifer. Indeed, this map schematises the reservoir's driving function and the hydrodynamic comportment of the aquifer. In this study, the piezometric levels were determined using Castany's (1982) formula in the case of a free tablecloth:

$$H = Z - (P - H_m)$$

With: H: Piezometric level (m)
Z: Ground level or elevation of the natural terrain (m)
P: Measured depth (m)
Hm: Coping height

3. RESULTS AND DISCUSSION

3.1 Results

3.1.1 Map of lineaments

The detailed network of lineaments extracted from radar images is shown in Fig. 8a. It consists of 9753 lineaments. Several lineaments which could correspond to regional faults, were

mapped. Fig. 8b shows the map of greater than 9 km sizes lineaments. The distribution of these major lineaments is not homogeneous from the study area.

3.1.2 Statistical analysis of fracture networks

Statistical analysis of fractures determined the percentages in number and cumulative length of fractures. The distribution of fracturing expressed in number and cumulative length is not homogeneous. Three major orientations N-S; NW-SE and NE-SW emerge from Fig. 9. Three major directions also seem to emerge from this Fig. N0-10 (18%); N110-120 (12%) and N70-80 (13%), with percentages above 10%. The main direction is N-S which is the Submeridian direction.

3.1.3 Validation of the fracture map

3.1.3.1 By the existing geological structures

The analysis of the histogram from the radar images (Fig. 10 A) shows the NW-SE and NE-SW directions with a predominance of N-S directions. As for the histogram from photo-geology (Fig. 10 B), it shows the N50-60, N60-70 (NE-SW) and N130-140 (NW-SE) directions respectively. The histogram of the optical images (Fig. 10 C) also shows the N20-30, N30-40 (NE-SW) and N110-120, N130-140 (NW-SE) directions. These images hardly show the N0-10 directions which are dominant on the histogram of the 1A sentinel radar images.In any case, due to its precision and finesse, the use of radar images for mapping geological structures is advantageous in terms of extent and number. In addition, the relevance of radar images in the field of structural geology is essential and constitutes a major asset for the prospection of groundwater.

3.1.3.2 Well-lineament distance analysis

In the Lobo watershed, out of the 32 wells with significant flows, 37.5% are located at a distance between 12.05 m and 270.92 m from the major lineaments. The flow rates of these wells vary from5 and 30 m^3 / h. Nevertheless, some significant yield were observed at distances ranging from 551.36 to 1294.99 m from the major lineaments. In this zone, the average distance between the high yield boreholes and the major lineaments is 485.19 m. These lineaments could be fractures. The wells with an average yield have an average distance from the major lineaments of 803.89 m with a maximum of 2,992.06 m while the wells with low yield have an average distance of 1,607.26 m from the lineaments. major, with a maximum of 7,574.23 m (Fig. 11).

In this area, out of the 133 wells used, 68 of them, i.e. 51.9%, have low yield (Q <2.5 m^3 / h). These wells were mainly installed in the 1980s based mainly on the geomorphology of the area. The wells with medium and high yield represent 23.66% and 24.42% respectively. these wells have generally been carried out using

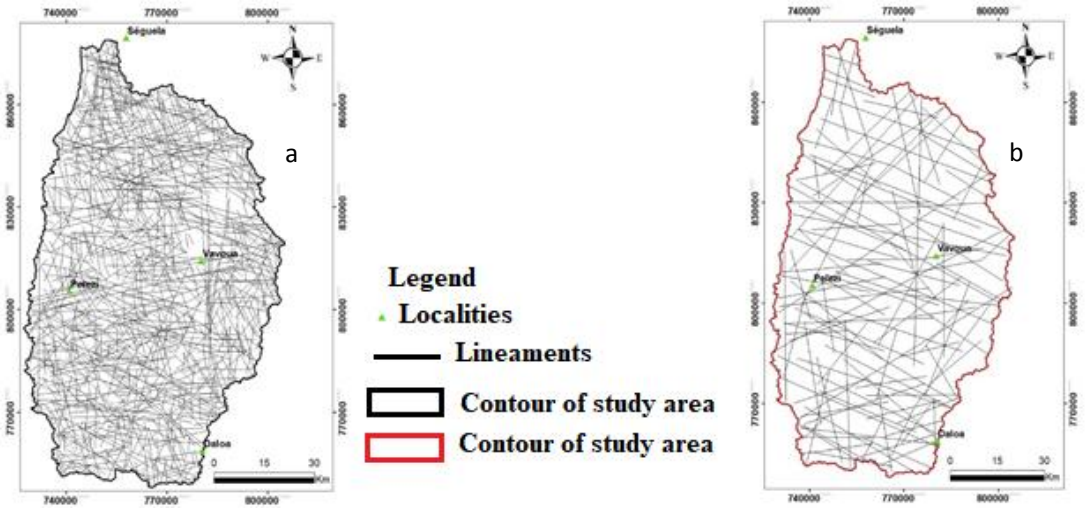

Fig. 8. Lineaments map of Lobo river basin a) detailed lineaments, b) major lineaments (length greater than 9 km)

geophysical methods. In this area, it emerges after analysis of these different results that the further the wells are from the lineaments, the lower the yield of these wells and vice versa. The wells with a flow rate (Q ≥ 5 m^3 / h) could then be located near or in the extension of a fracture. In the Lobo watershed, 40% of the wellswith a high yield (Q ≥ 5 m^3 / h) are located less than 300 m from the lineaments while 54.41% of those with a low yield (Q <2, 5 m^3 / h) are located more than 1000 m from lineaments. These major lineaments identified on the radar images could be fractures (Fig. 12).

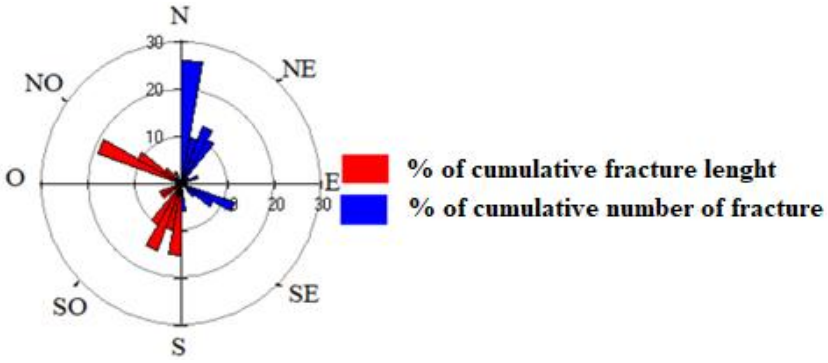

Fig. 9. Distribution of orientation frequencies in number and length of fractures

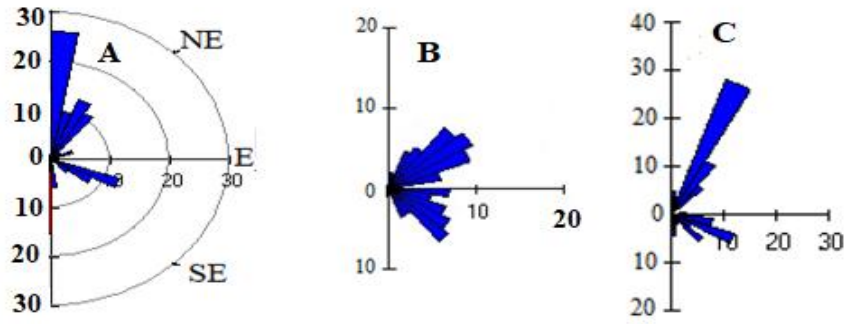

Fig. 10. Comparison of histograms: A) - from radar images; B) -; from optical images (Yao, 2015); C) - from the photogeological map (Biémi, 1992)

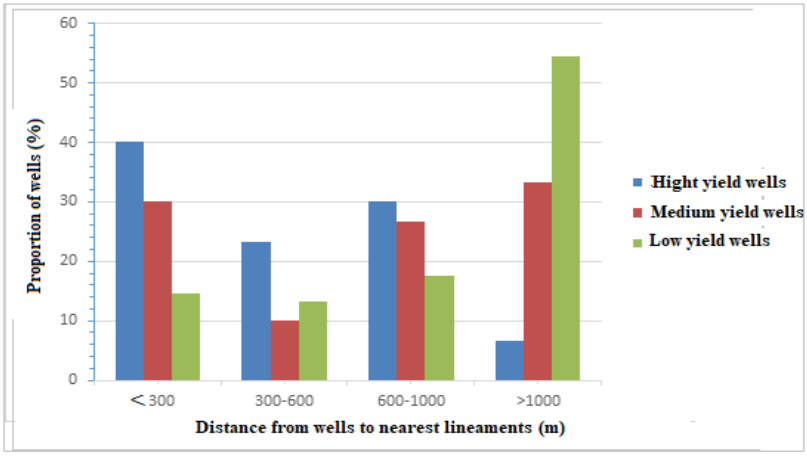

Fig. 11. Frequency distribution of implanted wells according to the distance from the nearest lineament

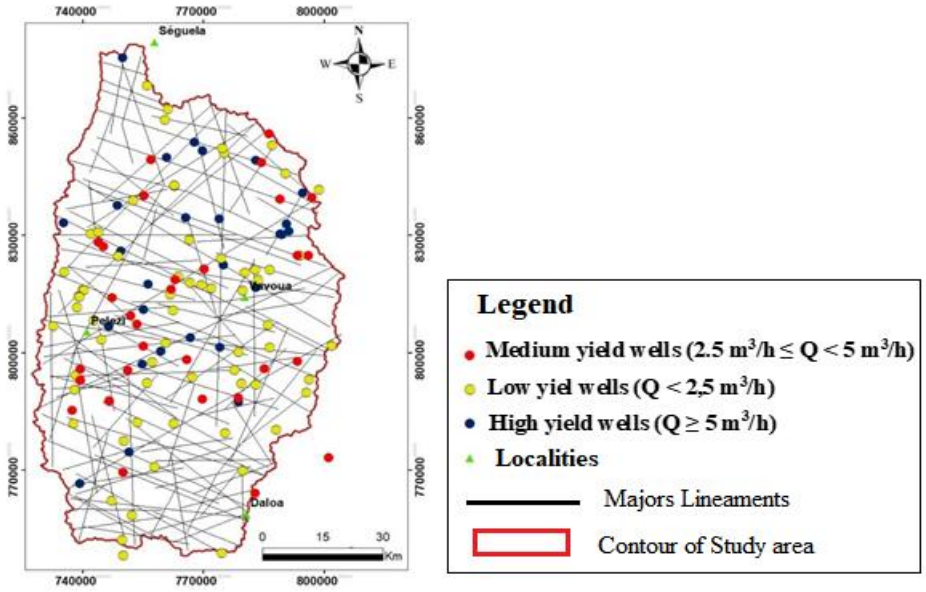

Fig. 12. Wells discriminated according to classes of yield and coupled with the major lineaments map

3.1.4 Intensity of fracturing

In order to better observe the spatial distribution of fracture density according to the number of fractures per unit area, we constructed the map of iso-values for the distribution of this parameter (Fig. 13a). The fractures are distributed differently over the entire study area. An overall analysis of this map shows that the Lobo catchment area is densely fractured and would therefore be conducive to good infiltration. Indeed, the middle, strong and very strong classes represent about 92% of the study area. On the other hand, areas with low fracture densities occupy about 8% of the study area. Nevertheless, it should be pointed out that the areas with very high fracturing densities occupy about 25% of the surface of the basin and are scattered throughout the entire study area, but mainly in its northern and central part.

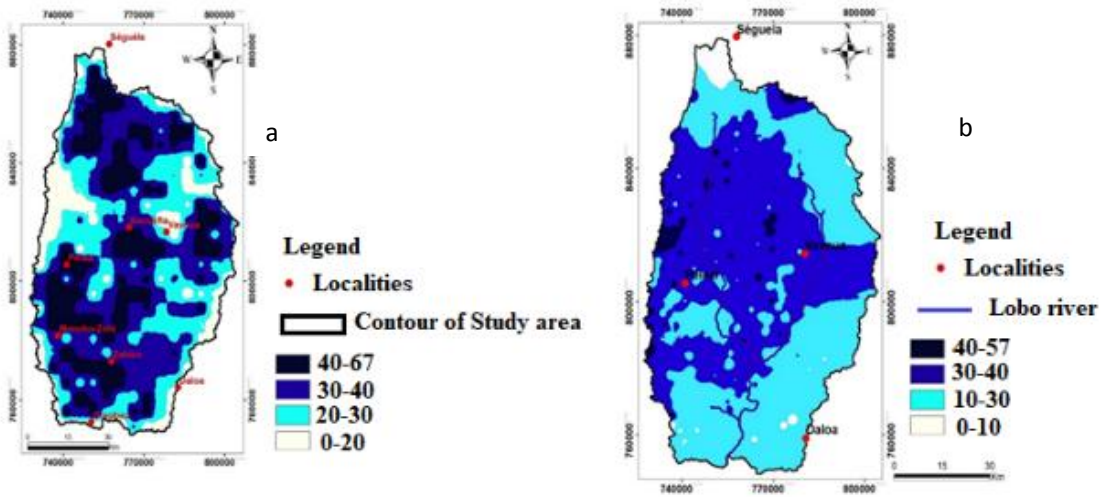

Fig. 13. Map of lineaments densities, a) cumulative length density (km/km²), b) cross-points density (n/km²)

3.1.5 Density of lineament crossing points

The spatial distribution map of the density of the lineament crossing points is shown in Fig. 13b. This figure seems to be modelled on that of the cumulative lengths of lineaments. This observation indicates a strong link between the crossing points of the lineaments and the lengths of the lineaments. Areas with high to very high densities of lineament crossing points would therefore be marked by the longest fractures and could constitute a real preferred flow area of groundwater. These observations clearly highlight the high fracturing density of the granitic rocks that occupy almost the entire study area. Similarly, medium to low density areas of lineament crossing points would be relatively more affected by the shortest fractures.

3.1.6 Preferential flow zone

In the Watershed of the Lobo river, groundwater generally flows in the same direction as surface water (north-south), which also corresponds to the main orientation of the fractures. In addition to heading towards the south of the basin, these groundwater are also directed towards the landfill areas of Mignoré, PK11 and Kétro-Bassam, which are characterised by a low topography. In this zone most of the boreholes with a flow rate greater than or equal to 5 m^3/h are located close to or in the extension of the preferential groundwater flow zone (Fig. 14). This zone could therefore be a favourable area for the installation of high-yield wells ($Q \geq 5$ m^3/h).This preferential flow zone, when it is superimposed on or close to the hydrographic network, favours the availability of the resource in all seasons in the bed of the watercourse (Fig. 15a), even if it may dry up in places (Fig. 15b).In this area, the preferential groundwater flow zone is almost superimposed on the hydrographic network. So this could confirm a groundwater-river interaction at these different locations on the Lobo River.

3.2 Discussion

The use of remote sensing for lineament mapping has been widely used around the world and in West Africa and significant results have been obtained [3,17,15,16,17,19]. These results made it possible to improve the success rate of wells in these areas. Sentinel 1A radar images, which are unaffected by atmospheric scattering and better suited to humid tropical areas such as the Lobo watershed, have enabled us to map the lineaments of this area. Statistical analysis of the mapped fracture network highlights different directional families of fractures. Thus, three major families of orientations were obtained; these are the N-S directions; NW-SE and NE-SW. These directions correspond to the Submeridian, Liberian and Eburnean directions respectively [14].These results are similar to those of [20] who worked in the Divo-Oumé region in the south-west of Côte d'Ivoire and obtained two major families of orientations (NW-SE and NE-SW).Among these identified orientations, some are close to the N40 direction considered by some authors as that of tension deformation. The directions who are close to him could be more productive, unlike directions such as E-W and NW-SE that are perpendicular to it. The E-W orientation is the least observed in the region. Indeed, the low occurrence of E-W fractures could be related to the effect of the direction of propagation of radar waves. These observations have also been made by [31, 32,19,7]. According to these authors, the E-W direction, in particular the N80-100 directions, would not be too visible in the radar images. In the Lobo watershed, of the 133 wells used in this study, 77% have flow rates of less than 5 m^3/hour. Most of these wells have been implanted more than 300 m from the fractures or on NW-SE or E-W oriented fractures. This could explain the high rate of low-yield drilling observed in the zone. However, the wells who is higth yield ($Q \geq 5$ m^3/h), of which there are 30, are for the most part close to fractures (less than 300 m) and are located on fractures with NE-SW directions with flow rates ranging from 5 to 30 m^3/h and N-S with flow rates ranging from 5 to 12 m^3/h.These fractures would be the result of tectonic events that affected the area. These complex tectonic phenomena that affected the region would have contributed to the development of a heterogeneous network of fractures. This network of fractures would be particularly very dense near rivers, which could encourage a significant outflow of water from the aquifer system towards the river, their valleys and the shallows. These areas (valleys and shallows) which could be groundwater discharge areas could also be areas for the establishment of future high-yield wells ($Q \geq 5$ m^3 / h). Holland M, Witthüser KT, [33], who worked in Limpopo Province in South Africa showed that rivers and their valleys are often associated with regional fractures. These assertions could justify the high density of fracturing observed in and near streams. This fracturing density favors in places the superimposition of the hydrogeological basin and the watercourse which could justify the availability of water resources in all seasons in

the bed of the river. Also, the Lobo watershed being mostly covered by granite rocks, this could help to explain this high density of fracturing. Indeed, [25] who worked in the department of Oumé showed that the fracturing of granite rocks would be more important than that of volcano-sedimentary rocks. This study also showed that the watershed is densely fractured at the level of the contact zones between the geological formations. This high density of fracturing in lithological contact zones has also been observed by several authors [7,34,19]. These areas could be suitable for the siting of future high yield wells.

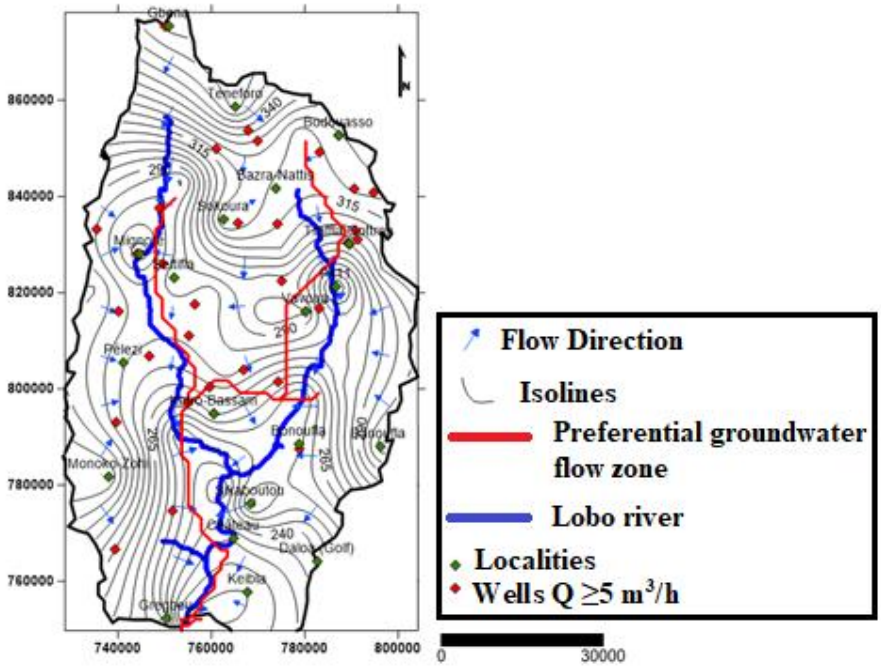

Fig. 14. Identification of the preferential groundwater flow area in the Watershed of the Lobo river

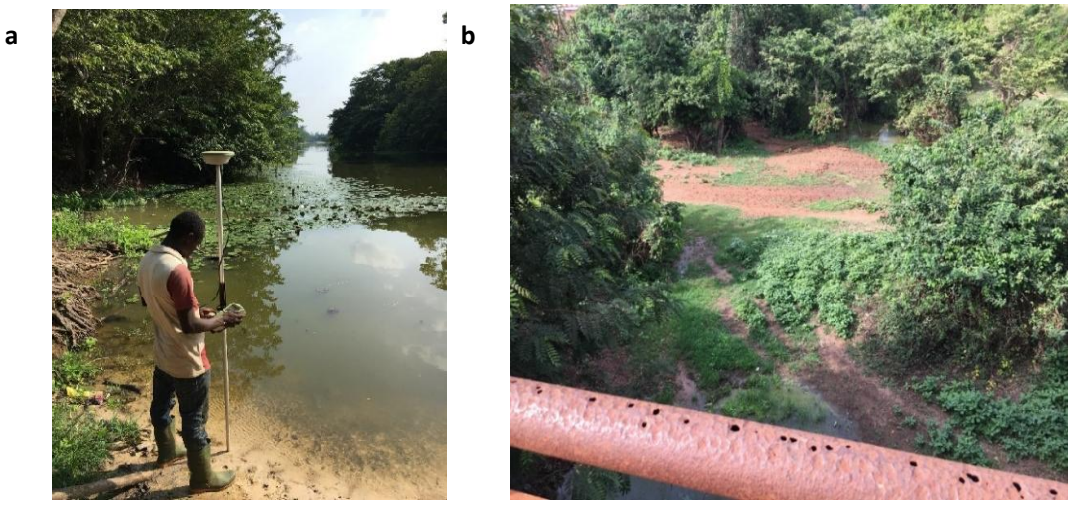

Fig. 15. Lobo river at the Sikaboutou hydrometric station in the dry season (a); Dry bed of the Lobo river in Mignoré the dry season (b) (February 2020)

4. CONCLUSION

The processing of sentinel 1A radar images made it possible to identify 9,753 lineaments including 121 major fractures with an average length of 9 km. The cumulative length of these fractures is 13,000 km over an area of 7,000 km². The main directions are: N-S - (N0-10), corresponding to the submeridian direction; NE-SW (N70–80), corresponding to Eburnean directions; NO-SE (N100-120), associated with the Liberian directions. In the Lobo watershed, the most productive wells are on average located less than 300 m from the fractures and are located on fractures near the N40 direction. In this zone, the study of the fracturing density and the number of fracture crossing points confirms the high fracturing density which varies from one zone to another due to the heterogeneity of the zone and is characterized by productivities variables. In the Lobo watershed, these fractures sometimes overlap the rivers. This river drains the aquifer.

COMPETING INTERESTS

Authors have declared that no competing interests exist.

REFERENCES

1. Calow RC, MacDonald AM, Nicol AL, Robins NS. Groundwater security and drought in Africa: linking availability access and demand. Ground Water; 2009. DOI: 10.1111 / j.1745-6584; 00558
2. Lachassagne P, Wyns R, Dewandel B. The fracture permeability of hard rock aquifers is due neither to tectonics, nor to unloading, but to weathering processes. Terra Nova. 2011;23(3):145–161.
3. DesRoches A, Danielescu S, Bulter K. Structural controls on groundwater flow in a fractured bedrock aquifer underlying an agricultural region of northwestern New Brunswick, Canada. Hydrogeol. J. 2014; 22:1067-1086.
4. Soro DD. Characterization and hydrogeological modeling of an aquifer in a fractured basement environment: Case of the sanon experimental site (central plateau region in Burkina Faso). Doctoral thesis, Pierre and Marie Curie University – Paris 6 (UPMC) - International Institute of Water and Environmental Engineering (2iE). 2017; 287.
5. Akinluyi FO, Olorunfemi MO, Bayowa OG. Investigation of the infuence of lineaments, lineament intersections and geology on groundwater yield in the basement complex terrain of Ondo State, Southwestern Nigeria. Appl. Water Sci. 2018;8(1):13-49.
6. Vassolo S, Neukum C, Tiberghien C, Hckmann M, Hahne K, Baranyikwa D. Hydrogeology of a weathered fractured aquifer system near Gitega, Burundi. Hydrogeol. J.; 2018. Available:https://doi.org/10.1007/s10040-018-1877-0
7. Biemi J. Contribution to the geological, hydrogeological and remote sensing study of the sub-Sahelian watersheds of the Precambrian basement of West Africa: Hydrostructural, hydrodynamics and isotopy of discontinuous aquifers of furrows and granite areas of the upper Marahoué (Côte ivory). Doctoral thesis in Natural Sciences, University of Abidjan. 1992;479.
8. Kouamé KF. Hydrogeology of discontinuous aquifers in the semi-mountainous region of Man-Danané (West of Côte d'Ivoire). Contribution of data from satellite images and statistical and fractal methods to the development of a hydrogeological information system with spatial reference. 3rd cycle doctoral thesis. Univ. Cocody. Abidjan, Ivory Coast). 1999; 194.
9. Lasm T, Kouamé KF, Oga MS, Jourda JRP, Soro N, Kouadio HB. Study of the productivity of fractured reservoirs in basement zones. Case of the Archean nucleus of Man Danané (West of Côte d'Ivoire), Revue Ivoirienne des Sciences et Technologie. 2004;5(97):1-15.
10. Saley MB, Kouamé KF, Penven MJ, Biémi J, Kouadio BH. Mapping of areas at risk of flooding in the semi-mountainous region at l 'West of Côte d'Ivoire: Contribution of unaccompanied minors and satellite imagery. Remote sensing. 2005;(4):277–288.
11. Adiaffi B. Contribution of isotope geochemistry, hydrochemistry and remote sensing to the knowledge of aquifers in the "basement-sedimentary basin" contact zone of south-eastern Côte d'Ivoire. Doctoral thesis, Paris-Sud University, France. 2008;196.

12. Corgne S, Magagi R, Yergeau M, Sylla D. An integrated approach to hydrogeological lineament mapping of a semi-arid region of West Africa using Radarsat-1 and GIS. Remote Sens. About. 2010;114:1863–1875.
13. Mangoua O, MJ. Assessment of the potential and vulnerability of groundwater resources in fissured aquifers in the Baya watershed (East of Côte d'Ivoire). Unique doctoral thesis, University of Abobo-Adjamé, Abidjan (Ivory Coast). 2013;169.
14. Yao AB. Assessment of the water potentials of the lobo watershed for rational management (Center-West of Côte d'Ivoire). Doctoral Thesis, Nangui Abrogoua University (Abidjan, Ivory Coast). 2015;225.
15. Assatse WT, Nouck PN. Tabod CT, Akame JM, Biringanin GN. Hydrogeological activity of lineaments in Yaounde´ Cameroon region using remote sensing and GIS techniques. Egypt. J. Remote Sens. Space Sci. 2016; 19:49–60.
16. Takorabt M, Toubal AC, Haddoum H, Zerrouk S. Determining the role of lineaments in underground hydrodynamics using Landsat 7 ETM + data, case of the Chott El Gharbi Basin (western Algeria). Arabian Journal of Geosciences. 2018 11(76):1-19.
17. Mangoua MJ, Kouassi KA, Douagui GA, Savané I, Biémi J. remote sensing and gis contribution for groundwater mapping reservoirs in the Baya Watershed (Eastern Region of Côte d'Ivoire). Journal of Geography, Environment and Earth Science International. 2019;23(3):1-14.
18. Ouédraogo M. Characterization of basement aquifers for improving the productivity of village water wells in the upstream Bandama Blanc watershed (North of Côte d'Ivoire). Doctoral thesis, Paris-Sud University, France. 2016;284.
19. Tagnon BO, Assoma TV, Mangoua OMJ, Douagui GDA, Kouamé KF, Savané I. Contribution of SAR / RADARSAT -1 and ASAR / ENVISAT images to geological structural mapping and assessment of lineaments density in Divo-Oumé area (Côte d'Ivoire). The Egyptian Journal of Remote Sensing and Space Sciences. 2020;3:231-241.
20. Wade, S., Ndoye, A., Mbaye, M. Fusion d'images optique et radar : application à la cartographie du massif granitique de Bambadji (Falémé, Sénégal oriental). Télédétection. 2 (2), 119–127. (2001).
21. Delor, C., Diaby, I., Yameogo, .S., Yao, B., Djama, A., Okou, A., Konaté, S., Taslet, J, P., Vidal, M., Traoré, I., Dommanget, A., Cauttu, J, P., Konan, G., Chiron, J, P. Carte Géologique de la Côte d'Ivoire à 1/200 000 ; Feuille Grand-Lahou, Mémoire de la Direction des Mines et de la Géologie, n°5, Abidjan, Côte d'Ivoire (1995).
22. Lee, J, S., Hoppel, K, W., Mango, S; A., Miller, A. Intensity and phase statistics of multiloock polarimetric interferometric SAR imagery. IEEE Trans. Geosci. Remote Sens. 32, 1017–1028 (1994).
23. Frost, V, S., Stiles, J, A., Josephine, A., Shanmugan, K; S., Holtzman, J, C. A model for radar images and its application to adaptive digital filtering of multiplicative noise. IEEE Trans. Pattern Anal. Machine Intell. (4) 157–166 (1982).
24. Haralick, S, Z. Image analysis using mathematical morphology. IEEE Trans. Pattern Anal. Machine Intell. PAMI-9. (4), 532–550 (1987).
25. Baka, D. Géométrie, hydrodynamisme et modélisation des réservoirs fracturés du socle protérozoïque de la région d'Oumé (Centre-Ouest de la Cote d'Ivoire). Thèse Unique, Univ. F.H. Boigny, Abidjan, Côte d'Ivoire. 249 p (2012).
26. Yao KT, Oga MS, Kouadio KE, Fouché O, Ferriere G, Pernelle C. Hydrogeological role of structural lineaments in crystalline and crystallophyllian medium: Case of the basin slope of Sassandra, southwest of Côte d'Ivoire. Africa Sci. 2014;10(4):78–92.
27. Jourda JP, Djagoua EV, Kouamé K, Saley BM, Gronayes C Achy JJ, Razack M. Identification and mapping of lithological units and major structural accidents of the Korhogo department (North of Côte d'Ivoire): Contribution of ETM + imagery from Landsat. Remote sensing. Flight. 2006;6(2):123-142.
28. Koita M. Characterization and modeling of the hydrodynamic functioning of a fractured aquifer in the basement zone: case of the region of Dimbokro-Bongouanou (Central East of Côte

d'Ivoire). Doctoral thesis, University of Montpellier 2, France. 2010;220.
29. Kim GO, Lee JY, Lee KK. Construction of lineament maps related to groundwater occurrence with ArcView and Avenue TM scripts. Computer Geosci. 2004;30:1117–1126.
30. Savané I, Goze B, Biémi J. Assessment of water resources in the basement by studying fractures using Landsat data (Odienné basin, Ivory Coast). Remote Sensing and Water Resources Management, FAO Colloquium, Montpellier; 1995.
31. Youan TM. Contribution of remote sensing and geographic information systems to hydrogeological prospecting of the Precambrian basement of West Africa: the case of the Bondoukou region (northeast of the Ivory Coast). Unique Thesis, University of Cocody (Ivory Coast). 2008; 237.
32. Raj NJ, Prabhakaran A, Muthukrishnan A. Extraction and analysis of geological lineaments of Kolli hills, Tamil Nadu: A study using remote sensing and GIS. Arab. J. Geosci. 2017;10:195–210.
33. Holland M, Witthüser KT. Evaluation of geologic and geomorphologic influences on borehole productivity in crystalline bedrock aquifers of Limpopo Province, South Africa. Hydrogeol. J. 2011;22(19):1062-1083.
34. Acharya T, Prasad R. Lithostratigraphic contact-a significant site for hydrogeological investigation in crystalline fractured-rock terrains. J. Earth Syst. Sci. 2017;126:15–28.

Peer-review history:
The peer review history for this paper can be accessed here:
http://www.sdiarticle4.com/review-history/63120